

Improving Generalized Born Models by Exploiting Connections to Polarizable Continuum Models. II. Corrections for Salt Effects

Adrian W. Lange[†] and John M. Herbert^{*}

Department of Chemistry and Biochemistry, The Ohio State University, Columbus, Ohio 43210, United States

ABSTRACT: A previous analytical investigation of the generalized Born (GB) implicit solvation model is extended to solvents of nonzero ionic strength. The GB model with salt effects (GB-SE) is shown to resemble the Debye–Hückel-like screening model (DESMO), a polarizable continuum model (PCM) that we have recently developed for salty solutions. DESMO may be regarded either as a generalization of the conductor-like PCM (C-PCM) that extends C-PCM to electrolyte solutions or alternatively as a generalization of Debye–Hückel theory to arbitrary cavity shapes. The connection between GB-SE and DESMO suggests how the former can be modified to account for the exclusion of mobile ions from the cavity interior, an effect that is typically absent in GB-SE models. We propose two simple GB-SE models that are exact for a point charge in a spherical cavity and that introduce the ability to account, albeit approximately, for the finite size of the mobile ions. The accuracy of these new models is demonstrated by applications to both model systems and real proteins. These tests also demonstrate the accuracy of the DESMO approach, as compared to more sophisticated PCMs developed for electrolyte solutions.

I. INTRODUCTION

Implicit solvent models, in various flavors,^{1–15} represent an efficient means to incorporate bulk solvent effects without the computational burden of an atomistic representation of the solvent. Most commonly, these models treat the solvent as a homogeneous dielectric medium, such that classical (continuum) electrostatics can be applied to compute the solvent reaction field arising from dielectric polarization by the solute.

In biomolecular and other macromolecular systems in aqueous solution, “mobile” ions from a dissolved electrolyte often have profound influence on structural and dynamical properties,^{16–21} so it is important to extend implicit solvent models to solvents with finite ionic strength. Assuming that the distribution of mobile ions is thermalized, the electrostatic interaction between the solute and the dielectric continuum is governed by the (nonlinear) Poisson–Boltzmann equation.^{5–7} When the relevant Boltzmann factors are truncated at first order, one obtains the *linearized* Poisson–Boltzmann equation (LPBE),²²

$$(\hat{\nabla}^2 - \kappa^2)U(\vec{r}) = 0 \quad (1.1)$$

where $U(\vec{r})$ is the total electrostatic potential. The LPBE assumes that the solvent is characterized by a dielectric constant (relative permittivity) denoted by ϵ and a Debye length λ that is related to the solvent’s ionic strength, I , according to

$$\kappa = \frac{1}{\lambda} = \left(\frac{8\pi e^2 I}{\epsilon k_B T} \right)^{1/2} \quad (1.2)$$

The quantity κ is known as the *inverse Debye screening length*. In this work, we will assume that the solute is separated from the dielectric medium by a sharp cavity boundary, with a dielectric constant of ϵ outside of the cavity and a dielectric constant of unity inside, the latter consistent with an explicit, atomistic treatment of electrostatics within the cavity. The theory could

be adapted for a different value of the dielectric constant within the cavity.²³

Methods of varying sophistication exist for solving either the linear or nonlinear Poisson–Boltzmann equation. Here, we focus on a class of methods known as *polarizable continuum models* (PCMs),¹⁴ or more specifically, “apparent surface charge” PCMs.^{13,14} In general, these models afford only an approximate solution for the solute polarization effects described by the LPBE, but they are computationally efficient as compared to three-dimensional volumetric integration of eq 1.1 and are furthermore exact in important special cases. PCMs of this sort are most often encountered in the context of electronic structure calculations (i.e., quantum-mechanical solutes), although they have recently become available for molecular mechanics applications within the Q-Chem software package.^{24–27} In this work, our aim is to connect these methods to variants of the generalized Born (GB) model,^{2,10,28,29} the most widely used implicit solvation model in classical biomolecular simulations.

Recently,³⁰ we presented a formal proof that the GB model, under certain reasonable assumptions, is equivalent to the so-called *conductor-like PCM* (C-PCM).³¹ This model is itself equivalent to the earlier “generalized COSMO” model,^{32,33} which is a slightly modified version of the original *conductor-like screening model* (COSMO) of Klamt and Schüürman,³⁴ one of the first PCMs to see widespread use. The GB/C-PCM equivalence rests on the following assumptions:³⁰

- (1) that the definition of the solute cavity is the same in both cases,
- (2) that the GB model uses “perfect” effective Born radii, and
- (3) that the pairwise *effective Coulomb operator* of GB theory is correct in the conductor limit.

Received: June 14, 2012

Published: August 21, 2012

The first assumption can be satisfied by construction. As for the second assumption, practical approximations can be found^{28,29,35–46} for the so-called perfect radii,⁴⁴ at least some of which appear to be quite accurate in practice.^{30,46} When perfect radii are used in the GB formalism, any error in the solvation energy is attributable solely to the choice of the effective Coulomb operator that is used in the pairwise-additive GB energy formula.³⁰ As such, it makes sense to insist on the correct conductor limit, since $\epsilon = 78.4$ (water) is not so far, in practice, from this limit.²⁶

In view of the aforementioned equivalence, C-PCM establishes a theoretical limit on the accuracy attainable from GB models, at least with regard to how well these models approximate the polarization energy obtained from Poisson's equation. Recently, we have introduced the *Debye–Hückel-like screening model* (DESMO),⁴⁷ which generalizes C-PCM/GCOSMO to solvents with nonzero ionic strength, within the approximation defined by the LPBE. (From another point of view, the DESMO approach extends the analytic Debye–Hückel theory,⁴⁸ which is valid only for spherical cavities, to a numerical theory that is valid for arbitrary cavity shapes.) The purpose of this work is to extend our analysis of the GB/C-PCM equivalence to a comparison between DESMO and the conventional GB model with salt effects (GB-SE).

For $\kappa > 0$, however, we are unable to demonstrate an *exact* mathematical equivalence between GB-SE and DESMO, but we are able to illustrate an *approximate* relationship between the two models, which holds up to numerical scrutiny as well. The similarity between the two models allows us to incorporate exclusion of the “mobile” (salt) ions into GB-SE models, in a manner similar to how ion exclusion is treated in DESMO. In previous GB-SE methods, ion exclusion is either lacking altogether or else is approximated by empirical scaling of κ .^{49,50}

Our presentation is organized as follows. After a brief review of the theory behind GB models and DESMO, we then develop a formal comparison between the two and show how the traditional GB-SE model fails to incorporate ion exclusion. This leads us to introduce a simple correction factor to account for this effect. Along these lines, we also propose an alternative form of GB-SE that is more efficient to compute, and which is exact for GB-SE self-energies although approximate for the pairwise energies. We next compare our proposed GB-SE models to some earlier ones in a series of tests on model systems, and also on a set of small proteins. Throughout this work, atomic units are used in the equations (so there is no $4\pi\epsilon_0$ in the Coulomb potential), but numerical results are presented in kcal/mol.

II. COMPARISON OF PCM AND GB THEORIES

A. Brief Review of Previous Work. We first review some important points from our previous study.³⁰ In GB models as well as PCMs, the total electrostatic energy of the solute + continuum system is partitioned into two contributions,

$$G_{\text{tot}} = G_0 + G_{\text{pol}} \quad (2.1)$$

where G_0 is the gas-phase electrostatic energy of the solute charge density, $\rho(\vec{r})$, and G_{pol} is the polarization energy arising from the interaction of $\rho(\vec{r})$ with the solvent reaction field. If $\rho(\vec{r})$ is comprised of atom-centered point charges,

$$\rho(\vec{r}) = \sum_i q_i \delta(\vec{r} - \vec{r}_i) \quad (2.2)$$

then the polarization energy can be written as a pairwise sum over atoms,

$$G_{\text{pol}} = \frac{1}{2} \sum_{i,j} G_{\text{pol},ij} \quad (2.3)$$

By the symmetry of the Coulomb interaction, $G_{\text{pol},ij} = G_{\text{pol},ji}$.

The decomposition in eq 2.3 is equally valid in both GB and PCM theory.³⁰ In the former case, we will denote the pairwise polarization energies as $G_{\text{pol},ij}^{\text{GB}}$, which can be equated with their PCM counterparts, $G_{\text{pol},ij}^{\text{PCM}}$, assuming that the same solute cavity is used in both models. Thus, we have

$$G_{\text{pol},ij}^{\text{GB}} = G_{\text{pol},ij}^{\text{PCM}} \quad (2.4)$$

with

$$G_{\text{pol},ij}^{\text{PCM}} = \int d\vec{s} \sigma_i(\vec{s}) \phi_j(\vec{s}) \quad (2.5)$$

The quantity $\sigma_i(\vec{s})$ is the portion of the total surface charge density at a point \vec{s} on the cavity surface that is induced by q_i , and $\phi_j(\vec{s})$ is the vacuum electrostatic potential at \vec{s} that is generated by q_j :

$$\phi_j(\vec{s}) = \frac{q_j}{|\vec{r}_j - \vec{s}|} \quad (2.6)$$

The total surface potential at \vec{s} is $\phi(\vec{s}) = \sum_i \phi_i(\vec{s})$, and the total surface charge density is $\sigma(\vec{s}) = \sum_i \sigma_i(\vec{s})$.

The simplest example of a PCM is obtained when the medium is a conductor ($\epsilon = \infty$), and this is a useful limit in the discussion below. In the conductor limit, the apparent surface charge PCM is defined by the equation

$$\hat{S}\sigma^{\text{cond}}(\vec{s}) = -\phi(\vec{s}) \quad (2.7)$$

where \hat{S} is a self-adjoint integral operator that maps a surface charge density onto the corresponding electrostatic potential,

$$\hat{S}\sigma(\vec{s}) = \int d\vec{s}' \frac{\sigma(\vec{s}')}{|\vec{s} - \vec{s}'|} \quad (2.8)$$

The C-PCM approach is “conductor-like” in the sense that its working equation is very similar to eq 2.7, differing only by an ϵ -dependent scaling of the total surface charge:

$$\hat{S}\sigma^{\text{C-PCM}}(\vec{s}) = (\epsilon^{-1} - 1)\phi(\vec{s}) \quad (2.9)$$

C-PCM is therefore exact in the conductor limit, and one expects that its accuracy should improve as ϵ increases. This expectation is borne out in numerical calculations.²⁶

B. Debye–Hückel-Like Screening Model. The primary working equation in DESMO that is solved for the apparent surface charge density is⁴⁷

$$\hat{S}\sigma^{\text{DESMO}}(\vec{s}) = \frac{\gamma(\vec{s})}{\epsilon} \phi^\kappa(\vec{s}) - \phi(\vec{s}) \quad (2.10)$$

This equation involves the screened electrostatic potential, ϕ^κ , arising from the solute charge density, $\rho(\vec{r})$. The screening involves the same attenuated Coulomb potential that appears in Debye–Hückel theory:

$$\phi^\kappa(\vec{s}) = \int d\vec{r} \rho(\vec{r}) \frac{e^{-\kappa|\vec{r}-\vec{s}|}}{|\vec{r} - \vec{s}|} \quad (2.11)$$

For a solute composed of classical point charges, we can rewrite eq 2.10 as an equation for σ_i ,

$$\hat{\sigma}_i^{\text{DESMO}}(\vec{s}) = \frac{\gamma(\vec{s})}{\epsilon} \phi_i^{\kappa}(\vec{s}) - \phi_i(\vec{s}) \quad (2.12)$$

with

$$\phi_i^{\kappa}(\vec{s}) = q_i \frac{e^{-\kappa|\vec{r}_i - \vec{s}|}}{|\vec{r}_i - \vec{s}|} \quad (2.13)$$

The quantity $\gamma(\vec{s})$ in eqs 2.10 and 2.12 is known as the *ion exclusion factor*,⁴⁷ because it alone accounts for the reduction in Debye screening that results from the fact that the “mobile” solvent ions are forbidden from penetrating the cavity interior. If ion exclusion is ignored altogether ($\gamma \equiv 1$), then one is effectively permitting an unphysical scenario in which some mobile ion charge density exists within the cavity interior. Note, however, that in the salt-free limit ($\kappa \rightarrow 0$), one does obtain $\gamma(\vec{s}) \equiv 1$. DESMO reduces to C-PCM in the same limit, and becomes exact in the limit $\epsilon \rightarrow \infty$. DESMO is also exact, independent of ϵ , for the model problem of a point charge centered in a spherical cavity, the same model considered by Debye and Hückel.⁴⁸

For more complex cavity shapes, a practical complication is that the exact function $\gamma(\vec{s})$ is not available (or, at least, is very complicated). This led us to propose a *local ion-exclusion layer* (LIEL) approximation for use with DESMO.⁴⁷ This approach is exact in the case of a point charge centered in a spherical cavity but approximate in other cases. For a point \vec{s} on the i th atomic sphere (whose radius is denoted R_i), the LIEL approximation amounts to an ion exclusion factor of the form

$$\gamma^{\text{LIEL}}(\vec{s}) = \frac{(1 + \kappa R_{\text{ion}}) e^{\kappa R_i}}{1 + \kappa(R_i + R_{\text{ion}})} \quad \text{for } \vec{s} \in i \quad (2.14)$$

Here, R_{ion} is the radius of the mobile ions, which are assumed to be identical. (The quantity R_{ion} defines the thickness of the *Stern layer* that surrounds the solute cavity.)

In ref 47, we showed that the LIEL approximation is significantly more accurate than simply ignoring ion exclusion altogether ($\gamma \equiv 1$, an approximation that we previously dubbed “DESMO-0”). Hereafter, we will continue to use “DESMO” to refer to the general PCM given by eq 2.10, but when we discuss numerical results that invoke the LIEL approximation, we will refer to the model as DESMO-LIEL to distinguish it from DESMO-0, where ion exclusion is neglected.

C. Connection between GB-SE and DESMO. Assuming that the solute charge density is given by eq 2.2, the pairwise polarization energy between atoms i and j in DESMO is²³

$$G_{\text{pol},ij}^{\text{DESMO}} = - \int d\vec{s} \phi_i(\vec{s}) \hat{S}^{-1} \phi_j(\vec{s}) + \frac{1}{\epsilon} \int d\vec{s} \phi_i(\vec{s}) \hat{S}^{-1} \gamma(\vec{s}) \phi_j^{\kappa}(\vec{s}) \quad (2.15)$$

Let us rewrite eq 2.15 in a way that better facilitates comparison to GB theory. To do so, we exploit the charge density in the conductor limit, $\sigma^{\text{cond}}(\vec{s}) = -\hat{S}^{-1} \phi(\vec{s})$, to obtain

$$G_{\text{pol},ij}^{\text{DESMO}} = \int d\vec{s} \sigma_i^{\text{cond}}(\vec{s}) \frac{q_j}{|\vec{r}_j - \vec{s}|} - \frac{1}{\epsilon} \int d\vec{s} \sigma_i^{\text{cond}}(\vec{s}) \frac{q_j \gamma(\vec{s}) e^{-\kappa|\vec{r}_j - \vec{s}|}}{|\vec{r}_j - \vec{s}|} \quad (2.16)$$

Note that all of the dependence on κ is contained in the second term, which we call the *salt term*.

We are now in a position to relate DESMO to GB-SE. The first step is to recognize that the first term in eq 2.16 is just the pairwise polarization energy in a conductor,

$$G_{\text{pol},ij}^{\text{cond}} = \int d\vec{s} \sigma_i^{\text{cond}}(\vec{s}) \frac{q_j}{|\vec{r}_j - \vec{s}|} \quad (2.17)$$

In GB theory, the pairwise energy for a conductor is expressed as

$$G_{\text{pol},ij}^{\text{GB}} = - \frac{q_i q_j}{f_{ij}^{\infty}} \quad \text{for } \epsilon \rightarrow \infty \quad (2.18)$$

where, as in our previous study,³⁰ $1/f_{ij}^{\infty}$ denotes the effective Coulomb operator evaluated in the conductor limit. This operator can be related to PCM theory *exactly*.³⁰ It is given by

$$\frac{1}{f_{ij}^{\infty}} = - \int d\vec{s} \tilde{\phi}_i(\vec{s}) \hat{S}^{-1} \tilde{\phi}_j(\vec{s}) \quad (2.19)$$

where $\tilde{\phi}_i(\vec{s}) = |\vec{r}_i - \vec{s}|^{-1}$. For $i = j$ (the self-energy), eqs 2.18 and 2.19 can be used to compute perfect effective Born radii for arbitrary cavity shapes, by using C-PCM calculations to evaluate the integral in eq 2.19.³⁰

Perusing the equations above, it is tempting to want to “replace” $|\vec{r}_i - \vec{s}|^{-1}$ in eq 2.17 with $1/f_{ij}^{\infty}$, to provide an effective Coulomb interaction between the surface charge density $\sigma_i^{\text{cond}}(\vec{s})$ and the atomic point charge q_j . One is then further tempted to substitute $-q_i$ in place of $\int d\vec{s} \sigma_i^{\text{cond}}(\vec{s})$ in eq 2.17, which is akin to applying Gauss’ law to the i th atom in the conductor limit to arrive at a uniformly distributed total effective surface charge. These replacements would have the effect of converting eq 2.17 into the form of eq 2.18, albeit not in a mathematically rigorous way.⁵¹ [For example, eq 2.19 suggests that $1/f_{ij}^{\infty}$ should depend in some way on cavity shape, but one ignores this dependence in decoupling $1/f_{ij}^{\infty}$ from $\sigma_i^{\text{cond}}(\vec{s})$ in the integrand of eq 2.17.]

However, applying the aforementioned substitutions to eq 2.16 does allow us to construct a model, which we may then attempt to rationalize and ultimately validate with numerical calculations. According to this model, the pairwise-additive GB-SE energy takes the form

$$G_{\text{pol},ij}^{\text{GB-SE}} = - \frac{q_i q_j}{f_{ij}^{\infty}} \left[1 - \frac{\gamma_{ij}}{\epsilon} \exp(-\kappa f_{ij}^{\infty}) \right] \quad (2.20)$$

where we have also replaced $\gamma(\vec{s})$ in eq 2.16 with γ_{ij} . Equation 2.20 is the *ansatz* that serves as a starting point for the GB-SE models developed in this work. A crucial aspect of these models is the choice of *ion exclusion factors*, γ_{ij} , which is discussed in section III. We note also that a somewhat more sophisticated form of GB theory developed by Onufriev and co-workers,^{50,52} known as the GB ϵ model, could be modified analogously, insofar as GB ϵ replaces $(f_{ij}^{\infty})^{-1}$ with a factor $(1 + \alpha/\epsilon)^{-1} [(f_{ij}^{\infty})^{-1} + \alpha/\epsilon A]$, where α and A are additional parameters. The same substitution can, if desired, be applied to the model in eq 2.20. This is discussed further in section III.B.

Substitution of eq 2.19 into eq 2.20 does *not* yield eq 2.16 exactly, so we have not established any rigorous mathematical equivalence between DESMO and GB-SE. Nevertheless, the resemblance between the two is uncanny. Note that in the limit $\kappa \rightarrow 0$, eq 2.20 reduces to the conventional salt-free pairwise GB energy. DESMO reduces to C-PCM in the same limit, as discussed above. As such, we anticipate that when the salt

concentration is low (the regime in which the LBPE is appropriate), the GB-SE model suggested in eq 2.20 may be similar to DESMO.

Further arguments in favor of the model defined by eq 2.20 can be made by considering two limiting cases that GB theory is intended to capture correctly. First, consider the case of a single point charge, q_i , centered in a sphere of radius R_i . In this case, the conductor surface charge is uniformly distributed, $\sigma_i^{\text{cond}}(\vec{s}) = -q_i/\int d\vec{s}$, where the denominator is simply the cavity surface area. Furthermore, for this special case, one has $|\vec{r}_i - \vec{s}| = R_i$, and $\gamma(\vec{s})$ is a constant that we denote by γ_{ii} . Under these conditions, eq 2.16 becomes

$$G_{\text{pol},ii}^{\text{DESMO}} = -\frac{q_i^2}{R_i} \left[1 - \frac{\gamma_{ii}}{\epsilon} \exp(-\kappa R_i) \right] \quad (2.21)$$

This expression does indeed have the form of eq 2.20, provided that $1/(f_{ii}^{\infty}) = R_i^{-1}$.

Next, consider the case of two charges q_i and q_j located at \vec{r}_i and \vec{r}_j , centered in disjoint spherical cavities whose radii are R_i and R_j , respectively. Let the two charges be sufficiently well separated, so that $|\vec{r}_i - \vec{r}_j| \gg R_i + R_j$. In this case, the surface charge $\sigma_i^{\text{cond}}(\vec{s})$ induced by q_i is confined to the surface of the i th sphere, and from the vantage point of \vec{r}_j , it should appear that $\sigma_i^{\text{cond}}(\vec{s}) \approx -q_i$, because this is the total surface charge on sphere i according to Gauss' law. Since $\sigma_i^{\text{cond}}(\vec{s}_j) \approx 0$ for any point \vec{s}_j on the surface of sphere j , we may neglect the integration over the surface of sphere j in eq 2.16. Given the separation of the charges, we can also approximate $|\vec{r}_i - \vec{s}_j| \approx |\vec{r}_i - \vec{r}_j|$, and furthermore $\gamma(\vec{s})$ becomes some constant, which we will call γ_{ij} . (This last point requires that the separation between the spheres is large compared to the radius of the mobile ions, but for $|\vec{r}_i - \vec{r}_j| \gg R_i + R_j$ this is a realistic approximation.) Putting this all together, eq 2.16 becomes

$$G_{\text{pol},ij}^{\text{DESMO}} \approx -\frac{q_i q_j}{r_{ij}} \left[1 - \frac{\gamma_{ij}}{\epsilon} \exp(-\kappa r_{ij}) \right] \quad (2.22)$$

This should be a good approximation when $r_{ij} = |\vec{r}_i - \vec{r}_j| \gg R_i + R_j$. Comparison to the model in eq 2.20 therefore suggests that $f_{ij}^{\infty} \rightarrow r_{ij}$ in the limit that $r_{ij} \gg R_i + R_j$.

The two limits established by these special cases are

$$f_{ij}^{\infty} \rightarrow r_{ij} \text{ as } r_{ij} \rightarrow \infty \quad (2.23a)$$

$$f_{ij}^{\infty} \rightarrow R_i \text{ as } r_{ij} \rightarrow 0 \quad (2.23b)$$

In fact, these are precisely the two limits in which the exact effective Coulomb operator is known analytically.³⁰ In particular, for $r_{ij} = 0$, eq 2.23b affords the correct result for a charge centered in a sphere. The model defined by eq 2.20 therefore has the correct form in these two important limits. As such, we could have arrived at eq 2.20 by first considering these two limits, then asking how one might interpolate between them within a GB-like formalism. The answer is to introduce a function f_{ij}^{∞} that interpolates between R_i and r_{ij} . It remains, however, to define the ion exclusion factors γ_{ij} . This is the topic of the next section.

III. ION EXCLUSION

A. Traditional GB-SE Models. Let us consider the importance of ion exclusion in eq 2.20. If we take $\gamma_{ij} = 1$, then we recover the traditional equation for GB-SE, which we will call GB-SE0:

$$G_{\text{pol},ij}^{\text{GB-SE0}} = -\frac{q_i q_j}{f_{ij}^{\infty}} [1 - \epsilon^{-1} \exp(-\kappa f_{ij}^{\infty})] \quad (3.1)$$

This equation was obtained previously by Srinivasan et al.⁴⁹ without any notion of DESMO or any other PCM. (In addition, the derivation in ref 49 does not make explicit the fact that the effective Coulomb operator should be evaluated in the conductor limit, which only becomes clear once the connection to C-PCM is made.) The notation GB-SE0 reflects an analogy to a method that we have previously termed DESMO-0,⁴⁷ in which $\gamma(\vec{s}) \equiv 1$. As discussed above, this approximation ignores the fact that the mobile solvent ions of Debye–Hückel theory should be prevented from penetrating into the interior of the solute cavity. Numerical calculations reveal that the DESMO-0 approximation overestimates salt effects,⁴⁷ consistent with additional screening arising from the mobile ion density within the solute cavity.

Srinivasan et al.⁴⁹ recognized that eq 3.1 also overestimates salt effects, as compared to numerical solution of the LPBE, and speculated that this might be due to the fact that there is no concept of ion exclusion in eq 3.1. To compensate, they propose to scale κ , which is determined by eq 1.2, by an empirical factor of 0.73. (This type of empirical screening has also been adopted to extend the GB ϵ model to salty solutions.⁵⁰) Replacing κ by 0.73κ reduces the Debye screening of the Coulomb interaction and is equivalent, in the present notation, to using eq 2.20 with ion exclusion factors

$$\gamma_{ij}^{\text{scale}} = \exp(0.27\kappa f_{ij}^{\infty}) \quad (3.2)$$

We will refer to the GB-SE model of eq 2.20, with ion exclusion factors defined by eq 3.2, as the GB-SE(scaled) model.

It is important to emphasize that eq 3.1—with or without empirical scaling—does not provide the correct energy for a point charge centered in a spherical cavity, nor does it incorporate any concept of a finite radius for the mobile ions. In fact, the polarization energy can be computed exactly from the LPBE for a point charge q_i centered in a spherical cavity, taking full account of ion exclusion. This is precisely the model problem solved by Debye and Hückel.⁴⁸ For a cavity of radius R_i and mobile ions of radius R_{ion} , the result is^{47,48}

$$G_{\text{pol}}^{\text{DH}} = -\frac{q_i^2}{2R_i} \left[1 - \frac{1}{\epsilon} \left(\frac{1 + \kappa R_{\text{ion}}}{1 + \kappa R_i + \kappa R_{\text{ion}}} \right) \right] \quad (3.3)$$

It is informative to expand the factor in parentheses as a Taylor series about $\kappa = 0$:

$$G_{\text{pol}}^{\text{DH}} = -\frac{q_i^2}{2R_i} \{ 1 - \epsilon^{-1} [1 - \kappa R_i + \kappa^2 (R_i^2 + R_i R_{\text{ion}}) + O(\kappa^3)] \} \quad (3.4)$$

Applying the GB-SE0 model [eq 3.1] to this same problem, recognizing that $f_{ii}^{\infty} = R_i$ [eq 2.23b], one obtains

$$G_{\text{pol}}^{\text{GB-SE0}} = -\frac{q_i^2}{2R_i} \left\{ 1 - \epsilon^{-1} \left[1 - \kappa R_i + \frac{1}{2} \kappa^2 R_i^2 + O(\kappa^3) \right] \right\} \quad (3.5)$$

This result agrees with the exact Debye–Hückel solution through $O(\kappa)$, as noted previously.^{2,49} However, since these previous treatments did not consider ion exclusion, it bears

pointing out that agreement through $O(\kappa)$ holds regardless of the value of R_{ion} . Finite ion size enters the Debye–Hückel formula only at $O(\kappa^2)$.

On the other hand, the empirical scaling suggested by Srinivasan et al.⁴⁹ affords the following approximation for the Debye–Hückel polarization energy:

$$G_{\text{pol}}^{\text{GB-SE(scaled)}} = -\frac{q_i^2}{2R_i} \{1 - \gamma_{ii}^{\text{scale}} e^{-1} [1 - \kappa R_i + O(\kappa^2)]\} \quad (3.6)$$

The agreement with the exact result through $O(\kappa)$ is spoiled by empirical scaling.

Further consideration of the Debye–Hückel model problem demonstrates that the electrostatic potential $u(r)$ at a distance $r \geq R_i + R_{\text{ion}}$ from the center of the sphere is^{47,48}

$$u(r) = \frac{q_i \exp[\kappa(R_i + R_{\text{ion}} - r)]}{\epsilon r [1 + \kappa(R_i + R_{\text{ion}})]} \quad (3.7)$$

Recasting this as

$$u(r) = \frac{q_i \gamma^{\text{DH}}}{\epsilon} \frac{e^{-\kappa r}}{r} \quad (3.8)$$

where

$$\gamma^{\text{DH}} = \frac{\exp[\kappa(R_i + R_{\text{ion}})]}{1 + \kappa(R_i + R_{\text{ion}})} \quad (3.9)$$

defines both the screened Coulomb operator ($e^{-\kappa r}/r$) and the ion exclusion factor (γ^{DH}) for Debye–Hückel theory.

In Figure 1, we plot the ratios $\gamma_{ii}^{\text{scale}}/\gamma^{\text{DH}}$ and $1/\gamma^{\text{DH}}$ as functions of κR_i . These two ratios provide a measure of how the

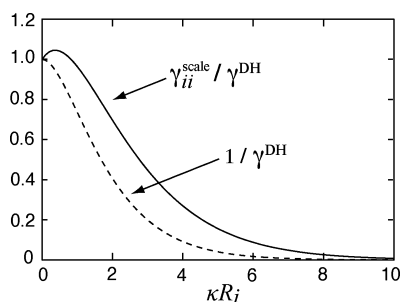


Figure 1. Relative error in the ion exclusion factor used in the GB-SE0 and GB-SE(scaled) methods, as compared to the exact Debye–Hückel result. The system consists of a point-charge solute centered in a spherical cavity, with $R_{\text{ion}} = 0$. Note that $\gamma_{ii} \equiv 1$ for the GB-SE0 model.

ion exclusion factors for the GB-SE(scaled) and GB-SE0 models, respectively, deviate from the exact result, for a point charge in a spherical cavity. In the case of GB-SE0, this deviation is rapid and significant, despite the fact that the model is correct through $O(\kappa)$. The GB-SE(scaled) result remains close to the Debye–Hückel result (that is, $\gamma_{ii}^{\text{scale}}/\gamma^{\text{DH}} \approx 1$) for somewhat larger values of κR_i , but its accuracy drops off sharply for values of $\kappa R_i \gtrsim 1.5$.

The lack of agreement between these GB-SE models and the exact Debye–Hückel result is unsatisfactory from a theoretical perspective but can be remedied in a straightforward fashion. Recognizing that DESMO is exact for the Debye–Hückel model problem, and comparing eq 2.10 for DESMO to eq 2.20 for GB-SE, it is clear that one must set

$$\gamma_{ii} = \gamma^{\text{DH}} \quad (3.10)$$

to ensure that GB-SE reduces to the correct Debye–Hückel solution in the limit $r_{ij} \rightarrow 0$. (For nonspherical cavities, we assume that the radius R_i that appears in γ^{DH} is the effective Born radius for atom i .) For $i \neq j$, the best choice for γ_{ij} is not so obvious and in fact need not be a constant, since $\gamma(\vec{s})$ depends on cavity shape. Nevertheless, we propose the following very simple generalization of eq 3.10:

$$\gamma_{ij} = (\gamma_{ii} + \gamma_{jj})/2 \quad (3.11)$$

The rationale for selecting an arithmetic average over, say, a geometric mean is discussed in the Appendix. Note that the factors $\gamma_{ii}/2$ can be computed outside of the pairwise GB loop, so that the computational overhead associated with ion exclusion is minimal. We will refer to eq 2.20, with γ_{ij} as defined in eqs 3.10 and 3.11, as the GB-SE γ model.

Finally, we propose an alternative way to incorporate ion exclusion into GB-SE that is designed to reduce the computational cost. As in our previous efforts to accelerate traditional GB calculations,³⁰ the goal is to avoid the costly exponential function that appears in eq 2.20. However, we wish to retain the Debye–Hückel limiting case for the self-energy. Our proposal is to write the GB-SE pairwise energy as [cf. eq 3.3]

$$G_{\text{pol},ij}^{\text{GB-SE(alt)}} = -\frac{q_i q_j}{f_{ij}^{\infty}} \left(1 - \frac{1 + \kappa R_{\text{ion}}}{\epsilon(1 + \kappa f_{ij}^{\infty} + \kappa R_{\text{ion}})} \right) \quad (3.12)$$

We refer to this model as GB-SE(alt). The computational simplification as compared to eq 2.20 should be readily apparent. Although the self-energies $G_{\text{pol},ii}^{\text{GB-SE(alt)}}$ are exact for the limiting Debye–Hückel case, the pairwise interactions $G_{\text{pol},ij}^{\text{GB-SE(alt)}}$ are screened slightly less than they should be (cf. eq 2.22). However, upon Taylor expansion of eq 3.12 about $\kappa = 0$, the GB-SE(alt) model is found to agree with eq 2.22 through $O(\kappa)$; hence we might expect this model to be reasonably accurate for low salt concentrations.

Consider GB-SE(alt) in comparison with the GB-SE0 model defined by eq 3.1, which is also correct through $O(\kappa)$ for the Debye–Hückel model problem. The GB-SE0 formula should be accurate for distal pairwise interactions but correct only to $O(\kappa)$ for the self-energy ($i = j$) terms. For GB-SE(alt), the opposite is true: this model is exact for the self-energy but correct only to $O(\kappa)$ for distal pairwise interactions. If one is content with errors of $O(\kappa^2)$, then GB-SE(alt) is a much better choice than GB-SE0 because it is computationally more efficient, and it has the ability to incorporate finite size for the mobile ions. We have found that, when carefully coded, $G_{\text{pol},ij}^{\text{GB-SE(alt)}}$ can be computed roughly 50% faster than $G_{\text{pol},ij}^{\text{GB-SE0}}$, as a result of eliminating the exponential function call.

B. GB-SE Models. So far, we have considered electrolytic extensions of the conventional GB model. As mentioned above, however, Onufriev and co-workers have introduced a somewhat more sophisticated GB model that they call GB ϵ .⁵² Later, the GB ϵ model was generalized to include salt effects, and this new model (which might be called GB ϵ -SE, in the language of the present work) was termed the *analytical linearized Poisson–Boltzmann* (ALPB) model.⁵⁰ The ALPB model was obtained by modifying the traditional GB *ansatz* based on consideration of Kirkwood’s analytic solution for an arbitrary multipolar distribution inside of a spherical cavity.⁵³ The resulting pairwise

polarization energy expression, including the correction for salt effects, is⁵⁰

$$G_{\text{pol},ij}^{\text{ALPB}} = \frac{-q_i q_j}{1 + \alpha/\epsilon} \left(1 - \frac{e^{-\kappa f_{ij}^\infty}}{\epsilon} \right) \frac{1}{F_{ij}^\infty} \quad (3.13)$$

where

$$\frac{1}{F_{ij}^\infty} = \frac{1}{f_{ij}^\infty} + \frac{\alpha}{\epsilon A} \quad (3.14)$$

The quantities α and A are discussed below. Consistent with the rest of this work, we assume a dielectric constant of unity inside of the cavity, although eq 3.13 is easily modified to lift this restriction. In addition, we have introduced f_{ij}^∞ into eq 3.13, which is not a part of the original ALPB model. Based upon the relevant asymptotic limits that ALPB is meant to capture, however, it is clear that this is appropriate.

The (nonadjustable) parameter α in eq 3.13 is a key part of the ALPB derivation,^{50,52} and is meant to approximate the factors of $l/(l+1)$ that appear (for $l > 1$) in the infinite summation over multipole moments, l , in Kirkwood's analytic model.⁵³ As such, α is a constant bounded between 1/2 and 1. Onufriev and co-workers have suggested a value of $\alpha \approx 0.571412$ for general purposes based on a thorough "first principles" error minimization.^{50,52} The variable A in eq 3.13 is known as the *electrostatic size* of the solute cavity and for a spherical cavity is equal to the cavity radius. For more complicated cavity shapes, approximations for A are employed.⁵⁰

Focusing on salt effects in the ALPB model, we note that in the limit $\alpha/\epsilon \rightarrow 0$, eq 3.13 reduces to eq 3.1, where the latter defines the model that we call GB-SE0. This suggests that eq 3.13 does not account for ion exclusion and is therefore incorrect even for the Debye–Hückel model problem. To amend this, one might choose to replace κ with 0.73κ , a procedure that was used in ref 50. Such empiricism, however, feels counter to the underlying *ab initio* spirit in which the ALPB model was derived and in any case does not afford the correct solution to the Debye–Hückel model problem.

As an alternative, we propose to modify the ALPB model along the same lines used to obtain the GB-SE γ and GB-SE(alt) models proposed above. We therefore introduce an "ALPB γ " model in which Debye–Hückel ion exclusion factors are introduced into eq 3.13:

$$G_{\text{pol},ij}^{\text{ALPB}\gamma} = \frac{-q_i q_j}{1 + \alpha/\epsilon} \left(1 - \gamma_{ij} \frac{e^{-\kappa f_{ij}^\infty}}{\epsilon} \right) \frac{1}{F_{ij}^\infty} \quad (3.15)$$

The factors γ_{ij} are defined by eqs 3.10 and 3.11, as in the GB-SE γ model. A more computationally expedient version of eq 3.15 is

$$G_{\text{pol},ij}^{\text{ALPB(alt)}} = \frac{-q_i q_j}{1 + \alpha/\epsilon} \left(1 - \frac{1 + \kappa R_{\text{ion}}}{\epsilon(1 + \kappa f_{ij}^\infty + \kappa R_{\text{ion}})} \right) \frac{1}{F_{ij}^\infty} \quad (3.16)$$

The ALPB γ and ALPB(alt) models introduced here each afford the correct solution for the Debye–Hückel model problem and reduce to the GB-SE γ and GB-SE(alt) models, respectively, in the limit $\alpha/\epsilon \rightarrow 0$. The accuracy of these proposed modifications to the ALPB model are examined numerically in section IV.C.

IV. NUMERICAL TESTS

A. Computational Details. We next turn to testing the GB-SE variants in comparison to PCMs. Rather than focusing on absolute polarization energies as a gauge of accuracy, we will focus on salt shifts

$$\Delta G(\kappa) = G_{\text{pol}}(\kappa) - G_{\text{pol}}(0) \quad (4.1)$$

We limit our tests to $\epsilon = 78.4$, corresponding to water at room temperature, and $\lambda = \kappa^{-1} = 3 \text{ \AA}$, corresponding (at room temperature) to a $\sim 1 \text{ M}$ solution of monovalent ions. Note that typical physiological ionic strengths are much smaller, typically 0.1–0.2 M,⁵⁴ corresponding to $\lambda \sim 8 \text{ \AA}$ at room temperature. Lower salt concentrations will reduce the salt effects, relative to those reported here, but the higher salt concentration provides a more rigorous test of the GB-SE models.

The various GB-SE models introduced above will be compared to PCM results using DESMO,⁴⁷ and also to the "screened" (finite ionic strength) version^{22,55,56} of the so-called *integral equation formalism* (IEF-PCM).^{55–58} The screened IEF-PCM constitutes an exact solution to the LPBE (within numerical discretization error) so long as $R_{\text{ion}} = 0$ and provided that the solute charge density is contained entirely within the cavity. (The latter assumption is satisfied trivially here, since we only consider solutes composed of classical point charges.⁵⁹)

We employ the switching/Gaussian (SWIG) discretization procedure for the PCM calculations,^{24,25} which is available in the Q-Chem software package.²⁷ We have recently extended the SWIG approach to compute analytical matrix elements for the screened IEF-PCM.⁴⁷ For the ion-pair model that is considered in section IV.B, the cavity consists simply of two spheres, but for the proteins in section IV.D we employ Connolly's "solvent excluded" cavity surface definition,⁶⁰ with a solvent probe radius of 1.4 \AA , appropriate for water. The average grid resolution of the discretized surfaces is 0.07 \AA^2 per surface element. Matrix inversion, rather than iterative methods, is used to solve the discretized version of eq 2.9.

The protein data set used in section IV.D is identical to the "small protein training set" of ref 30, and details can be found in Appendix C of that work. For all test systems, perfect effective Born radii are obtained from C-PCM calculations, as described previously,³⁰ and are then used in the GB calculations. In practical applications, it is necessary to employ fast analytic expressions for approximate Born radii,^{29,35–37,40–43} which do not require volumetric integration and yield analytic forces for molecular dynamics. In our previous work on GB models,³⁰ however, we showed that numerical results show only very small differences if one substitutes so-called R6* radii⁴⁶ in place of perfect radii. The R6* radii are derived from a much-simplified integral procedure⁴⁵ and are efficient enough to be used in much larger macromolecules. Analytic forces could probably be obtained by application of appropriate switching functions, as in the SWIG discretization approach. This remains a topic for future work.

B. Ion-Pair Model. In this section, we consider the salt shift as a function r_{ij} for a system of two elementary charges ($q_i = q_j = +e$), each centered in a spherical cavity of radius 1.5 \AA . In the PCM calculations, the two spheres are allowed to interpenetrate (for $r_{ij} < 3 \text{ \AA}$) according to the SWIG method. For the GB-SE calculations, we use the "canonical" effective Coulomb operator introduced by Still et al.²⁸

$$f_{ij}^{\text{Still}} = \sqrt{r_{ij}^2 + R_i R_j} \exp(-r_{ij}^2 / 4R_i R_j) \quad (4.2)$$

As defined in ref 28, the quantity R_i is the *effective Born radius* for atom i , for which we use “perfect” radii.⁴⁴ These can be obtained from C-PCM calculations, and in particular from eq 2.19, since $f_{ii}^{\infty} = R_i^{\infty}$ is the perfect radius.³⁰

We first consider the case in which solvent mobile ions are assumed to have negligible size ($R_{\text{ion}} = 0$). Salt shifts obtained using various GB-SE models are plotted in Figure 2 along with

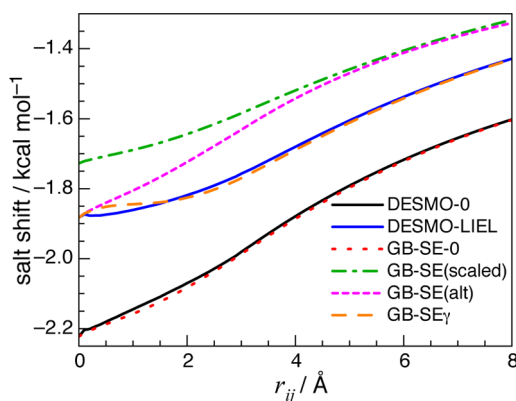


Figure 2. Salt shifts for two solute charges separated by a distance r_{ij} for mobile ions of negligible size ($R_{\text{ion}} = 0$). For $r_{ij} < 3 \text{ \AA}$, the spherical cavities around the two charges interpenetrate.

DESMO-LIEL and DESMO-0 results. We find that the theory developed above is predictive of the observed trends. GB-SE0 agrees very closely with DESMO-0, both of which overestimate the magnitude of the salt shift relative to more accurate⁴⁷ DESMO-LIEL results. The empirically scaled result is incorrect at $r_{ij} = 0$, as expected, but in fact differs from the DESMO-LIEL result by a roughly constant shift across a broad range of r_{ij} . The DESMO-LIEL, GB-SE(alt), and GB-SE γ models all obtain the exact result at $r_{ij} = 0$. However, GB-SE(alt) diverges from DESMO-LIEL as the distance increases, although it is no worse than GB-SE(scaled). GB-SE γ is clearly the most accurate of the GB-SE variants and is nearly identical to the DESMO-LIEL result except for very small deviations around $r_{ij} \approx 0.5 \text{ \AA}$.

Results are plotted in Figure 3 for the less common case in which solvent mobile ions are assumed to have finite size, namely, $R_{\text{ion}} = 2 \text{ \AA}$. DESMO-0, GB-SE0, and GB-SE(scaled)

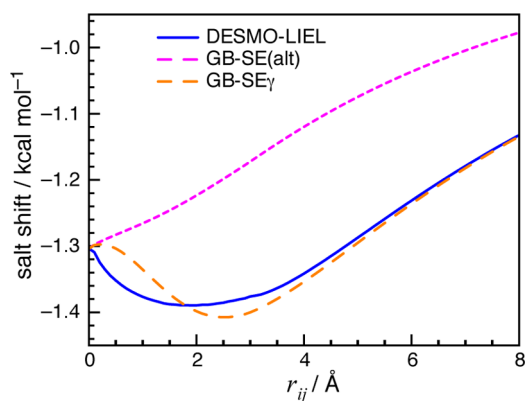


Figure 3. Salt shift for two solute charges separated by a distance r_{ij} with a mobile ion radius $R_{\text{ion}} = 2 \text{ \AA}$. For $r_{ij} < 3 \text{ \AA}$, the spherical cavities around the two charges interpenetrate.

results are not shown, since these methods do not incorporate ion exclusion and thus would predict the same salt shifts as when $R_{\text{ion}} = 0$; those shifts would be at least 0.5 kcal/mol too large, in the present example. For the methods that *do* incorporate ion exclusion, the trends are quite similar to those observed when $R_{\text{ion}} = 0$. For distances $r_{ij} > 3 \text{ \AA}$, where the two spherical cavities are disjoint, the GB-SE γ and DESMO-LIEL salt shifts are practically indistinguishable, whereas the GB-SE(alt) salt shift differs by an approximately constant offset. At shorter distances, where the spheres interpenetrate, discrepancies between GB-SE γ and DESMO-LIEL are slightly larger, but all three methods converge to the exact result for $r_{ij} = 0$, as expected.

C. GB ϵ -SE for a Spherical Cavity. Next, consider a collection of point charges in a spherical cavity of radius A , centered at the origin. For this special case, there are a number of simple analytic formulas for GB models that we utilize here. In the limit $\epsilon \rightarrow \infty$, the perfect radius associated with the i th charge is⁴⁵

$$R_i^{\infty} = A - r_i^2/A \quad (4.3)$$

where A is the radius of the sphere and r_i is the distance between the i th charge and the center of the sphere. The so-called R6 radii are exact [equal to R_i^{∞} from eq 4.3] in this special case.⁴⁵ In addition, the effective Coulomb operator

$$f_{ij}^{\text{sphere}} = \sqrt{r_{ij}^2 + R_i R_j} \quad (4.4)$$

is exact in the limit $\epsilon \rightarrow \infty$, provided that $R_i = R_i^{\infty}$ from eq 4.3.⁴⁵ In other words, these two formulas together yield f_{ij}^{∞} (eq 2.19) for spherical cavities.

We now investigate numerical results for the “sphere-15 \AA ” test system of Onufriev and co-workers, which was used in ref 52 to test the GB ϵ model. This system consists of a spherical solute cavity centered at the origin with a radius $A = 15 \text{ \AA}$, in which the solute is 11 point charges (with $q_i = +e$ for each), located at Cartesian coordinates $(\pm 6 \text{ \AA}, 0, 0)$, $(0, \pm 6 \text{ \AA}, 0)$, $(0, 0, 6 \text{ \AA})$, $(\pm 12 \text{ \AA}, 0, 0)$, $(0, \pm 12 \text{ \AA}, 0)$, and $(0, 0, \pm 12 \text{ \AA})$. For the ALPB models discussed in section III.B, the parameter A is simply the cavity radius, and we use $\alpha = 0.571412$ as recommended by Onufriev and co-workers.^{50,52} Born radii are obtained from eq 4.3 and the effective Coulomb operator from eq 4.4, to ensure that we have an exact f_{ij}^{∞} in these tests. DESMO and IEF-PCM calculations are performed using a Lebedev grid with 5294 points, for an average grid resolution of 0.534 \AA^2 . As in the other tests, $\epsilon = 78.4$ and $\lambda = 3 \text{ \AA}$. Ion exclusion is ignored in this example ($R_{\text{ion}} = 0$).

Numerical results for the aforementioned test system are listed in Table 1. The IEF-PCM approach affords an exact result up to discretization error, which should be quite small given the grid resolution. The DESMO-LIEL results use a modified version of the LIEL approximation (eq 2.14) in which $R_i = 6 \text{ \AA}$ rather than 15 \AA . The latter choice leads to significant error because the solute charges are not centered in the spherical cavity, a deficiency in the LIEL approximation that was noted in our previous work.⁴⁷ The radius $R_i = 6 \text{ \AA}$ used to compute the ion exclusion factors was selected as the average distance to the cavity surface for solute charges located at $(-6 \text{ \AA}, 0, 0)$ and $(-12 \text{ \AA}, 0, 0)$. As such, the DESMO-LIEL results are not as rooted in first principles as other options, but this choice does reduce errors in the salt shift, as compared to DESMO-0 results that overestimate the salt shift.

Table 1. Total Polarization Energies (G_{pol}) and Salt Shifts (ΔG) for the “sphere-15 Å” Test System of Ref 52, in kcal/mol

method	G_{pol}		ΔG	error ^a
	$\kappa = 0$	$\kappa = (3 \text{ \AA})^{-1}$		
IEF-PCM	-1377.58	-1392.20	-14.62	0.00
DESMO-0	-1378.15	-1395.08	-16.93	-2.31
DESMO-LIEL ^b	-1378.15	-1393.80	-15.65	-1.03
ALPB ^c	-1377.76	-1395.04	-17.28	-2.66
ALPB(scaled) ^d	-1377.76	-1394.50	-16.74	-2.12
ALPB γ ^e	-1377.76	-1393.61	-15.85	-1.23
ALPB(alt) ^f	-1377.76	-1392.19	-14.43	0.19

^aError in ΔG with respect to the IEF-PCM result. ^bModified LIEL approximation using $R_i = 6 \text{ \AA}$. ^cEquation 3.13. ^dEquation 3.13 with κ replaced by 0.73κ . ^eEquation 3.15. ^fEquation 3.16.

The ALPB method (eq 3.13) is very accurate for the salt-free case, exhibiting even better agreement with IEF-PCM than DESMO in the limit $\kappa \rightarrow 0$. We note that if we let $\alpha = 0$ in ALPB for the tests with $\kappa = 0$, the resulting polarization energy ($G_{\text{pol}} = -1378.17 \text{ kcal/mol}$) equals the C-PCM polarization energy with negligible error, as predicted by the formal C-PCM/GB equivalence.

For the salty case ($\lambda = 3 \text{ \AA}$), the ALPB methods in Table 1 differ as a result of different treatments of ion exclusion. The original ALPB method (eq 3.13), which ignores ion exclusion altogether, overestimates the salt shift by an amount comparable to DESMO-0. Empirical scaling (replacing κ with 0.73κ) reduces this error only slightly. Our proposed modifications to ALPB, however, show a much more appreciable improvement, especially ALPB(alt), where the results are nearly in agreement with IEF-PCM results. These results suggest that ALPB calculations can be improved by corrections for ion exclusion, which should be considered in future tests for nonspherical cavities.

D. Protein Data Set. Finally, we consider a set of 16 small proteins that are more representative of the type of systems for which GB-SE methods are typically used. Although GB results for small sets of macromolecules may not always be representative of the performance for larger data sets,²⁹ this is the same data set that we recently used to assess GB and C-PCM results in the salt-free case.³⁰ Previous work on salt-free GB models has suggested that the effective Coulomb operator employed by Still et al.²⁸ (eq 4.2) may not be the optimal choice,^{30,61} and for calculations on the protein data set we employ an alternative operator

$$f_{ij}^{\text{p16}} = r_{ij} + \sqrt{R_i R_j} \left(1 + \frac{\zeta r_{ij}}{16 \sqrt{R_i R_j}} \right)^{-16} \quad (4.5)$$

where $\zeta = 1.028$ is an empirical parameter. This so-called “p16” operator was introduced in ref 30 and shown to be slightly more accurate than f_{ij}^{still} , both for the data set considered here (which was used to optimize ζ , in the salt-free calculations of ref 30) and also for a larger data set of proteins and nucleic acids. If implemented carefully,³⁰ f_{ij}^{p16} is also less expensive to evaluate, by as much as a factor of 3 relative to f_{ij}^{still} .

We initially chose to use f_{ij}^{p16} here because it was the most accurate of the analytic effective Coulomb operators that we tested in ref 30. However, we have repeated the GB-SE calculations in this section using f_{ij}^{still} , and we find that while the absolute polarization energies obtained using f_{ij}^{still} are indeed less accurate than those computed using f_{ij}^{p16} , as judged by comparison to exact IEF-PCM results, the salt shifts obtained using either operator are remarkably similar, differing by $\lesssim 0.1 \text{ kcal/mol}$.

For comparison, we also report GB-SE salt shifts using the exact effective Coulomb operator, f_{ij}^{∞} , which can be computed from C-PCM calculations for each atom pair, using eq 2.19. (Analytic models such as f_{ij}^{p16} and f_{ij}^{still} are thus compromise choices intended to mimic the data set of pairwise f_{ij}^{∞} values.³⁰)

Table 2. Protein Salt Shifts (in kcal/mol) for Mobile Ions of Negligible Size, $R_{\text{ion}} = 0$

PDB code	PCMs			GB models using f_{ij}^{p16}				GB models using f_{ij}^{∞}			
	DESMO-LIEL	DESMO-0	IEF-PCM	GB-SE0	GB-SE (scaled)	GB-SE (alt)	GB-SE γ	GB-SE0	GB-SE (scaled)	GB-SE (alt)	GB-SE γ
1AJJ	-5.32	-5.83	-5.56	-6.22	-5.07	-4.90	-5.12	-6.31	-5.12	-5.02	-5.17
1BBL	-4.58	-5.16	-5.06	-5.37	-4.23	-4.37	-4.62	-5.59	-4.37	-4.65	-4.92
1BOR	-3.16	-3.76	-4.00	-3.92	-2.89	-3.19	-2.93	-4.03	-2.96	-3.32	-2.98
1BPI	-7.28	-7.90	-7.15	-8.11	-6.97	-6.80	-7.43	-8.25	-7.05	-6.98	-7.57
1CBN	-0.63	-0.86	-0.91	-0.93	-0.64	-0.82	-0.62	-0.97	-0.66	-0.88	-0.60
1FCA	-8.68	-9.27	-10.07	-9.39	-8.29	-7.84	-8.68	-9.49	-8.36	-7.94	-8.64
1FXD	-30.90	-31.94	-29.23	-32.24	-30.04	-27.17	-31.06	-32.33	-30.10	-27.28	-30.88
1HPT	-2.06	-2.62	-3.11	-2.74	-1.95	-2.35	-1.96	-2.93	-2.07	-2.56	-2.14
1MBG	-16.19	-16.89	-15.46	-17.28	-15.45	-14.14	-16.43	-17.52	-15.60	-14.42	-16.79
1PTQ	-10.58	-11.20	-10.05	-11.73	-10.33	-9.60	-10.66	-11.83	-10.38	-9.77	-10.87
1R69	-5.15	-5.74	-5.55	-5.99	-4.92	-4.96	-5.27	-6.14	-5.01	-5.14	-5.39
1SH1	-2.58	-3.09	-3.54	-3.34	-2.42	-2.71	-2.51	-3.45	-2.48	-2.84	-2.53
1UXC	-7.11	-7.74	-7.11	-7.98	-6.83	-6.71	-7.25	-8.17	-6.94	-6.99	-7.58
1VII	-3.70	-4.25	-4.66	-4.45	-3.40	-3.61	-3.74	-4.56	-3.46	-3.73	-3.86
1VJW	-7.59	-8.31	-8.71	-8.57	-7.24	-7.16	-7.68	-8.68	-7.31	-7.29	-7.67
2ERL	-6.33	-6.78	-6.14	-6.89	-6.16	-5.78	-6.34	-6.98	-6.21	-5.89	-6.38
MSD ^a	0.28	-0.31		-0.55	0.59	0.89	0.25	-0.62	0.58	0.79	0.21
MUD ^a	0.69	0.67		0.60	0.73	0.89	0.75	0.74	0.62	0.79	0.70
RMSD ^a	0.83	0.92		1.09	0.90	1.07	0.89	1.01	0.82	1.07	0.80

^aMean signed deviation (MSD), mean unsigned deviation (MUD), and root-mean-square deviation (RMSD) with respect to IEF-PCM calculations.

When f_{ij}^{∞} is employed, the salt-free GB energy expression exactly reproduces the C-PCM energy, by virtue of the GB/C-PCM equivalence.³⁰

Last, we have also performed screened IEF-PCM calculations for this data set, in order to gauge the accuracy of DESMO. For $R_{\text{ion}} = 0$, the screened IEF-PCM method affords the same polarization energy as the LPBE, without the need for the ion exclusion factors that are required for accuracy in DESMO calculations.⁴⁷ On the other hand, it is unclear how to generalize the IEF-PCM approach to account for mobile ions of finite size; hence, IEF-PCM calculations always tacitly assume that $R_{\text{ion}} = 0$. In addition, screened IEF-PCM calculations are significantly more expensive than DESMO calculations, and the IEF-PCM calculations reported here constitute the largest such calculations, of which we are aware, both in terms of molecular size (up to 997 atoms) and number of grid points (up to 45,328). Thus, they represent good benchmarks against which to compare DESMO for large systems.

Salt shifts computed for the protein data set are listed in Table 2 for the case $R_{\text{ion}} = 0$. Since screened IEF-PCM affords the exact result in this case, we also tabulate statistical deviations for each method with respect to IEF-PCM. Surprisingly, the DESMO-0 and DESMO-LIEL results are about equally accurate, statistically speaking, albeit with mean errors that tend in opposite directions. However, there is no evidence of *systematic* deviations in either case, as may be judged by the very similar mean unsigned errors (MUEs). The GB-SE models exhibit somewhat larger errors with respect to IEF-PCM, with the exception of the GB-SE γ model, whose performance is comparable to DESMO-LIEL. This is true when the exact effective Coulomb operator (f_{ij}^{∞}) is used, but also when f_{ij}^{p16} is used instead, which is important since f_{ij}^{∞} is time-consuming to compute and is therefore only useful as a benchmark.

Next, we compute protein salt shifts for the case that $R_{\text{ion}} = 2$ Å, using three methods that include corrections for ion exclusion; results are listed in Table 2. Whereas the IEF-PCM results are exact (up to discretization errors) when $R_{\text{ion}} = 0$, for mobile ions of finite size there exists no exact analytic result, to the best of our knowledge. We do note that statistical deviations between GB-SE(alt) and GB-SE γ results with respect to DESMO-LIEL are slightly larger in these cases than was observed for $R_{\text{ion}} = 0$, especially when the analytic Coulomb operator f_{ij}^{p16} is used rather than the exact f_{ij}^{∞} . Consistent with results for the ion-pair model (section IV.B), the GB-SE γ model affords results that are statistically closer to DESMO-LIEL as compared to GB-SE(alt).

Although *total* salt shifts predicted by the various GB-SE models are in fairly decent agreement with one another, more significant variations are observed if we decompose the salt shift into *self-energy* ($i = j$) and *pair-energy* ($i \neq j$) contributions. This is done in Table 3, using f_{ij}^{∞} with $R_{\text{ion}} = 0$. We expect that the self-energy contributions are most accurate for the GB-SE γ model, since this model affords the exact self-energy for the Deybe–Hückel model problem, whereas GB-SE0 is correct only through $O(\kappa)$. The GB-SE(alt) model has the same self-energies as GB-SE γ , by construction.

Compared to GB-SE γ , GB-SE0 clearly overestimates the magnitude of the self-energy contributions to the salt shift, by ~ 8 kcal/mol on average. The scaling introduced in eq 3.2 has the effect of reducing the magnitude of the self-energies (and the pair energies as well), and GB-SE(scaled) self-energies are significantly closer to GB-SE γ results.

Table 3. Protein Salt Shifts (in kcal/mol) for Mobile Ions of Size $R_{\text{ion}} = 2.0$ Å

PDB code	DESMO-LIEL	GB with f_{ij}^{p16}		GB models using f_{ij}^{∞}	
		GB-SE(alt)	GB-SE γ	GB-SE(alt)	GB-SE γ
1AJJ	-4.45	-3.60	-4.79	-3.66	-3.88
1BBL	-3.56	-3.10	-4.51	-3.24	-3.69
1BOR	-2.24	-2.12	-2.93	-2.19	-1.67
1BPI	-6.26	-5.33	-7.46	-5.42	-6.37
1CBN	-0.25	-0.49	-0.84	-0.52	-0.06
1FCA	-7.75	-6.36	-8.54	-6.42	-7.44
1FXD	-29.33	-23.40	-30.54	-23.45	-28.90
1HPT	-1.14	-1.48	-2.33	-1.59	-0.88
1MBG	-15.00	-11.59	-16.24	-11.73	-15.46
1PTQ	-9.54	-7.72	-10.49	-7.79	-9.53
1R69	-4.15	-3.68	-5.24	-3.77	-4.16
1SH1	-1.76	-1.75	-2.33	-1.81	-1.35
1UXC	-6.05	-5.25	-7.32	-5.37	-6.32
1VII	-2.79	-2.48	-3.51	-2.54	-2.77
1VJW	-6.39	-5.53	-7.16	-5.60	-6.17
2ERL	-5.64	-4.72	-6.27	-4.78	-5.49
MSD ^a		1.10	0.89	1.03	0.14
MUD ^a		1.18	0.89	1.22	0.26
RMSD ^a		1.88	0.93	1.83	0.32

^aDeviations with respect to DESMO-LIEL.

As for pair-energy contributions, these are also largest for the GB-SE0 model, and empirical scaling brings them closer to GB-SE γ values. Recall that this empirical scaling was introduced in the first place⁴⁹ based on the recognition that the model that we call GB-SE0 overestimates *total* salt effects. What does not seem to have been recognized in ref 49 is that GB-SE0 overestimates both the self-energy and pair-energy terms, by a fairly significant amount relative to GB-SE γ , yet because these terms have opposite sign, the discrepancies tend to cancel. The total salt shift evaluated using the GB-SE0 model is therefore not so different from the GB-SE γ result.

To a lesser extent, the same observations are true for the empirically scaled model, GB-SE(scaled): self-energies tend to be more negative than GB-SE γ results, but pair energies are more positive. However, these discrepancies largely cancel when the total salt shift is evaluated. The GB-SE(alt) pair energies, on the other hand, are quite close to GB-SE γ results (Table 4). Unlike the self-energy terms, which have the same form in GB-SE(alt) and GB-SE γ by construction, the fact that the pair energies are in good agreement is not guaranteed by the form of the model.

That the GB-SE0 model appears to exaggerate both self-energy and pair-energy contributions to the salt shift arises from the neglect of ion exclusion. Some sort of ion exclusion is included in the empirically scaled GB-SE(scaled) model, albeit in a roundabout way, yet self-energies and pair energies are still slightly exaggerated as compared to GB-SE γ results. It seems likely that the GB-SE0 and GB-SE(scaled) models may also overestimate forces that arise from the polarization energy, which is potentially a concern for molecular dynamics simulations based on these models. Although total salt shifts are quite similar among all of the GB-SE models considered here, GB-SE γ affords the correct result for the Debye–Hückel model problem without increasing the complexity of the basic GB-SE *ansatz*. The GB-SE(alt) model, which affords similar

Table 4. Decomposition of Protein GB-SE Salt Shifts (in kcal/mol), Using f_{ij}^{∞} and $R_{\text{ion}} = 0.0 \text{ \AA}$

PDB code	self-energy			pair energy			
	GB-SE0	GB-SE (scaled)	GB-SE γ^a	GB-SE0	GB-SE (scaled)	GB-SE (alt)	GB-SE γ
1AJJ	-28.14	-23.16	-22.45	21.83	18.04	17.43	17.28
1BBL	-33.80	-27.36	-27.34	28.21	22.99	22.69	22.42
1BOR	-39.58	-32.61	-31.66	35.55	29.65	28.34	28.67
1BPI	-45.01	-37.05	-36.02	36.76	30.00	29.04	28.45
1CBN	-31.00	-25.54	-24.68	30.03	24.88	23.81	24.08
1FCA	-37.95	-31.17	-30.22	28.46	22.81	22.28	21.59
1FXD	-46.29	-37.95	-37.04	13.96	7.85	9.76	6.15
1HPT	-47.99	-39.40	-38.42	45.07	37.33	35.86	36.28
1MBG	-44.33	-36.63	-35.36	26.81	21.03	20.94	18.57
1PTQ	-37.17	-30.67	-29.69	25.33	20.30	19.92	18.82
1R69	-50.84	-42.08	-40.55	44.70	37.07	35.41	35.17
1SH1	-34.66	-28.64	-27.57	31.22	26.16	24.73	25.04
1UXC	-42.40	-34.71	-34.19	34.23	27.77	27.20	26.61
1VII	-28.91	-23.66	-23.15	24.35	20.20	19.42	19.29
1VJW	-42.16	-34.78	-33.58	33.47	27.48	26.29	25.92
2ERL	-31.65	-25.90	-25.31	24.67	19.69	19.42	18.93

^aGB-SE(alt) self-energies are identical to those for GB-SE γ , by construction.

self-energies and pair energies as compared to GB-SE γ , actually reduces the complexity of this *ansatz*.

V. CONCLUSIONS

We have investigated the generalization of GB theory to electrolytic solvents, in comparison to the Debye–Hückel-like screening model⁴⁷ (DESMO) that generalizes the well-established C-PCM method^{31–33} to solvents with nonzero ionic strength. The methodology of GB with salt effects (GB-SE), which is introduced here from a new theoretical perspective, bears considerable formal similarity to DESMO and, like DESMO, can be formulated in a way that has certain correct formal limits. This formal comparison facilitates development of simple corrections to improve traditional GB-SE models by accounting for the exclusion of mobile ions from the solute cavity, and a new model (called GB-SE γ) has been developed along these lines. Unlike previous GB-SE models,^{49,50} the GB-SE γ model does not invoke any empirical scaling of the Debye screening length.

Preliminary tests on a small set of proteins show that GB-SE γ performs well in comparison to DESMO calculations. Admittedly, the total salt shifts predicted by the GB-SE γ model are not considerably different from those obtained using the empirically scaled model of Srinivasan et al.⁴⁹ In a certain sense, this is a validation of GB-SE γ , since the empirically scaled model has been tested against grid-based finite-difference Poisson–Boltzmann solvers and found to yield similar trends in salt shifts for B-DNA.⁴⁹ Unlike GB-SE γ , however, the empirically scaled model is not exact for the Debye–Hückel model of a single charge in a spherical cavity, and salt shifts appear to result from error cancellation between exaggerated self-energies and pair energies, which have opposite signs. As such, the GB-SE γ approach is more appealing, from a theoretical point of view. In future work, we plan to perform extensive tests of these models against numerical Poisson–Boltzmann results.

Finally, we have proposed an alternative approach, GB-SE(alt), that avoids evaluating the exponential function and is therefore much less costly to evaluate as compared to other GB-SE methods, including GB-SE γ . By construction, the GB-SE(alt) model affords the exact self-energy for the Debye–

Hückel model problem and is correct through $O(\kappa)$ in the pair energies. Tests on a small set of proteins suggest that GB-SE(alt) is slightly less accurate as compared to GB-SE γ , but given its increased efficiency it may prove to be a useful tool for implicit solvent calculations of large biomolecules in aqueous environments with modest salt concentrations.

■ APPENDIX: COMBINATION RULES FOR γ_{ij}

We take γ_{ii} to be defined by the Debye–Hückel result [eq 3.10]. To define γ_{ij} for $i \neq j$, we seek a model with the following properties:

- γ_{ij} should be simple to compute.
- γ_{ij} should reduce to γ^{DH} for $i = j$.
- Reasonable accuracy should be obtained in other cases.

Computational simplicity suggests that we should consider choices that reuse γ_{ii} and γ_{jj} according to some combination rule, as is commonly done for the Lennard-Jones “sigma” parameters in molecular mechanics force fields. Three simple combination rules come to mind: the arithmetic, geometric, and harmonic means:

$$\gamma_{ij}^{\text{A}} = (\gamma_{ii} + \gamma_{jj})/2 \quad (\text{A.1a})$$

$$\gamma_{ij}^{\text{G}} = (\gamma_{ii}\gamma_{jj})^{1/2} \quad (\text{A.1b})$$

$$\gamma_{ij}^{\text{H}} = 2/(\gamma_{ii}^{-1} + \gamma_{jj}^{-1}) \quad (\text{A.1c})$$

Each of these is easy to compute and each reduces to γ_{ii} for $i = j$.

Here, we test the accuracy of these three combination rules for a model problem consisting of two point charges centered in disjoint spherical cavities. For $R_{\text{ion}} = 0$, Lotan and Head-Gordon (LHG) have derived an analytic solution to the LPBE for this model problem,⁶² and this solution suggests an approximation for the ion exclusion factor:

$$\gamma_{ij}^{\text{LHG}} \approx \gamma_{ii}\gamma_{jj} \quad (\text{A.2})$$

The accuracy of this approximation improves as the distance between the two cavities increases. This appears to be the limit that γ_{ij} should approach for large r_{ij} , but it is important to point

out that this is for the case of two ions fully exposed to the solvent dielectric. Interactions between charged species that are embedded well inside the solute cavity need not obey the same limit.

Equation A.2 creates a conundrum. This equation cannot be used as a combining rule because it does not afford the correct limit (γ^{DH}) for the case $i = j$. One could devise a formula to interpolate between γ^{DH} and γ_{ij}^{LHG} as a function of r_{ij} , but this only serves to complicate matters and reduce the efficiency of the GB-SE γ model, which is counter to the spirit of keeping GB models simple and efficient. Instead, we seek a compromise from eq A.1 that is most similar to γ_{ij}^{LHG} .

Let us set $\gamma_{ij} = \exp(\kappa R_i)/(1 + \kappa R_i)$, as usual [eq 3.9 for $R_{\text{ion}} = 0$], but set $\gamma_{ij} = \exp(a\kappa R_i)/(1 + a\kappa R_i)$, which is equivalent to setting $R_j = aR_i$ for some scalar, a . We then compute γ_{ij} according to the combining rules in eq A.1. In Figure 4, we plot

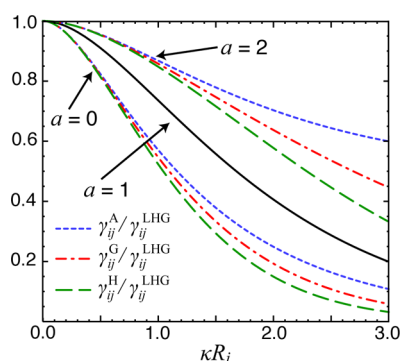


Figure 4. Ratios of γ_{ij} , computed using one of the combining rules in eq A.1, to the approximation LHG γ_{ij} defined in eq A.2, for two charges centered in well-separated spheres whose radii are R_i and $R_j = aR_i$, with $R_{\text{ion}} = 0$. For $a = 1$ (solid black curve), all three combining rules are equivalent.

the ratio of γ_{ij} obtained in this way to γ_{ij}^{LHG} , for $a = 0, 1$, and 2 . For $a = 1$, $\gamma_{ii} = \gamma_{jj}$ and all three combining rules are equivalent, and this case serves simply as a point of comparison for the cases where one sphere is larger than the other.

From Figure 4, we observe that all three ratios $\gamma_{ij}^X/\gamma_{ij}^{\text{LHG}}$ (for $X = A, G$, or H) converge to the proper limit as $\kappa R_i \rightarrow 0$. (The ion exclusion factors should all be unity for $\kappa = 0$.) For finite values of κR_i , however, the ratios $\gamma_{ij}^X/\gamma_{ij}^{\text{LHG}}$ differ from unity, and none of the three combining rules mimics γ_{ij}^{LHG} in an entirely satisfactory way. However, the ratio $\gamma_{ij}^A/\gamma_{ij}^{\text{LHG}}$ is closest to unity, for both $a = 0$ and $a = 2$. As such, we propose the arithmetic mean in eq 3.11 for computing γ_{ij} for the GB-SE γ model. The numerical tests in section IV demonstrate that this choice provides reasonable accuracy for realistic applications.

AUTHOR INFORMATION

Corresponding Author

*E-mail: herbert@chemistry.ohio-state.edu.

Present Address

[†]Argonne Leadership Computing Facility, Argonne National Laboratory, Argonne, IL 60439

Notes

The authors declare no competing financial interest.

ACKNOWLEDGMENTS

This work was supported by an NSF CAREER award (CHE-0748448). Calculations were performed at the Ohio Super-

computer Center (project no. PAS-0291). J.M.H. is an Alfred P. Sloan Foundation fellow and a Camille Dreyfus Teacher-Scholar. A.W.L. acknowledges a Presidential Fellowship from The Ohio State University.

REFERENCES

- (1) Warshel, A.; Papazyan, A. *Curr. Opin. Struct. Biol.* **1998**, *8*, 211–217.
- (2) Bashford, D.; Case, D. A. *Annu. Rev. Phys. Chem.* **2000**, *51*, 129–152.
- (3) Feig, M.; Brooks, C. L., III. *Curr. Opin. Struct. Biol.* **2004**, *14*, 217–224.
- (4) Baker, N. A. *Method. Enzymol.* **2004**, *383*, 94–118.
- (5) Baker, N. A. *Curr. Opin. Struct. Biol.* **2005**, *15*, 137–143.
- (6) Grochowski, P.; Trylska, J. *Biopolymers* **2008**, *89*, 93–113.
- (7) Lu, B. Z.; Zhou, Y. C.; Holst, M. J.; McCammon, J. A. *Commun. Comput. Phys.* **2008**, *3* (5), 973–1009.
- (8) Wang, J.; Tan, C.; Tan, Y.-H.; Lu, Q.; Luo, R. *Commun. Comput. Phys.* **2008**, *3*, 1010–1031.
- (9) Onufriev, A. *Annu. Rep. Comput. Chem.* **2008**, *4*, 125–137.
- (10) Onufriev, A. In *Modeling Solvent Environments: Applications to Simulations of Biomolecules*; Feig, M., Ed.; Wiley-VCH: Hoboken, NJ, 2010; Chapter 6, pp 127–165.
- (11) Marchand, F.; Caflisch, A. In *Modeling Solvent Environments: Applications to Simulations of Biomolecules*; Feig, M., Ed.; Wiley-VCH: Hoboken, NJ, 2010; Chapter 9, pages 209–232.
- (12) Yap, E.-H.; Head-Gordon, T. *J. Chem. Theory Comput.* **2010**, *6*, 2214–2224.
- (13) Chipman, D. M. *Theor. Chem. Acc.* **2002**, *107*, 80–89.
- (14) Tomasi, J.; Mennucci, B.; Cammi, R. *Chem. Rev.* **2005**, *105*, 2999–3093.
- (15) Cramer, C. J.; Truhlar, D. G. *Acc. Chem. Res.* **2008**, *41*, 760–768.
- (16) Marlow, G. E.; Perkyms, J. S.; Pettitt, B. M. *Chem. Rev.* **1993**, *93*, 2053–2521.
- (17) Record, T. M., Jr.; Zhang, W.; Anderson, C. F. *Adv. Protein Chem.* **1998**, *51*, 281–353.
- (18) Zhang, Y.; Cremer, P. S. *Curr. Opin. Struct. Biol.* **2006**, *10*, 659–663.
- (19) Zhang, Y.; Cremer, P. S. *Annu. Rev. Phys. Chem.* **2010**, *61*, 63–83.
- (20) Ciferri, A. *Chem.—Eur. J.* **2010**, *16*, 10930–10945.
- (21) Nostro, P. L.; Ninham, B. W. *Chem. Rev.* **2012**, *112*, 2286–2322.
- (22) Chipman, D. M. *J. Chem. Phys.* **2004**, *120*, 5566–5575.
- (23) Equation 2.15 assumes that the cavity interior has a dielectric constant $\epsilon_{\text{int}} = 1$ (i.e., vacuum dielectric). However, a different value of ϵ_{int} is easily incorporated simply by scaling the first term in eq 2.15 by $1/\epsilon_{\text{int}}$.
- (24) Lange, A. W.; Herbert, J. M. *J. Phys. Chem. Lett.* **2010**, *1*, 556–561.
- (25) Lange, A. W.; Herbert, J. M. *J. Chem. Phys.* **2010**, *133*, 244111:1–18.
- (26) Lange, A. W.; Herbert, J. M. *Chem. Phys. Lett.* **2011**, *509*, 77–87.
- (27) Shao, Y.; Fusti-Molnar, L.; Jung, Y.; Kussmann, J.; Ochsenfeld, C.; Brown, S. T.; Gilbert, A. T. B.; Slipchenko, L. V.; Levchenko, S. V.; O’Neill, D. P.; DiStasio, R. A., Jr.; Lochan, R. C.; Wang, T.; Beran, G. J. O.; Besley, N. A.; Herbert, J. M.; Lin, C. Y.; Van Voorhis, T.; Chien, S. H.; Sodt, A.; Steele, R. P.; Rassolov, V. A.; Maslen, P. E.; Korambath, P. P.; Adamson, R. D.; Austin, B.; Baker, J.; Byrd, E. F. C.; Dachsels, H.; Doerksen, R. J.; Dreuw, A.; Dunietz, B. D.; Dutoi, A. D.; Furlani, T. R.; Gwaltney, S. R.; Heyden, A.; Hirata, S.; Hsu, C.-P.; Kedziora, G.; Khalliulin, R. Z.; Klunzinger, P.; Lee, A. M.; Lee, M. S.; Liang, W.; Lotan, I.; Nair, N.; Peters, B.; Proynov, E. I.; Pieniazek, P. A.; Rhee, Y. M.; Ritchie, J.; Rosta, E.; Sherrill, C. D.; Simonnet, A. C.; Subotnik, J. E.; Woodcock, H. L., III; Zhang, W.; Bell, A. T.; Chakraborty, A. K.; Chipman, D. M.; Keil, F. J.; Warshel, A.; Hehre, W. J.; Schaefer, H. F., III; Kong, J.; Krylov, A. I.; Gill, P. M. W.; Head-Gordon, M. *Phys. Chem. Chem. Phys.* **2006**, *8*, 3172–3191.

- (28) Still, W. C.; Tempczyk, A.; Hawley, R. C.; Hendrickson, T. J. *Am. Chem. Soc.* **1990**, *112*, 6127–6129.
- (29) Lee, M. S.; Salsbury, F. R., Jr.; Brooks, C. L., III. *J. Chem. Phys.* **2002**, *116*, 10606–10614.
- (30) Lange, A. W.; Herbert, J. M. *J. Chem. Theory Comput.* **2012**, *8*, 1999–2011.
- (31) Barone, V.; Cossi, M. *J. Phys. Chem. A* **1998**, *102*, 1995–2001.
- (32) Truong, T. N.; Stefanovich, E. V. *Chem. Phys. Lett.* **1995**, *240*, 253–260.
- (33) Truong, T. N.; Nguyen, U. N.; Stefanovich, E. V. *Int. J. Quantum Chem., Symp.* **1996**, *30*, 1615–1622.
- (34) Klamt, A.; Schüürmann, G. *J. Chem. Soc., Perkin Trans. 2* **1993**, 799–805.
- (35) Hawkins, G. D.; Cramer, C. J.; Truhlar, D. G. *Chem. Phys. Lett.* **1995**, *246*, 122–129.
- (36) Hawkins, G. D.; Cramer, C. J.; Truhlar, D. G. *J. Phys. Chem.* **1996**, *100*, 19824–19839.
- (37) Schaefer, M.; Karplus, M. *J. Phys. Chem.* **1996**, *100*, 1578–1599.
- (38) Scarsi, M.; Apostolakis, J.; Caffisch, A. *J. Phys. Chem. A* **1997**, *101*, 8098–8106.
- (39) Ghosh, A.; Rapp, C. S.; Friesner, R. A. *J. Phys. Chem. B* **1998**, *102*, 10983–10990.
- (40) Qiu, D.; Shenkin, P. S.; Hollinger, F. P.; Still, W. C. *J. Phys. Chem. A* **1997**, *101*, 3005–3014.
- (41) Lee, M. S.; Feig, M.; Salsbury, F. R., Jr. *J. Comput. Chem.* **2003**, *24*, 1348–1356.
- (42) Lee, M. S.; Salsbury, F. R., Jr.; Olson, M. A. *J. Comput. Chem.* **2004**, *25*, 1967–1978.
- (43) Gallicchio, E.; Levy, R. M. *J. Comput. Chem.* **2004**, *25*, 479–499.
- (44) Onufriev, A.; Case, D. A.; Bashford, D. *J. Comput. Chem.* **2002**, *23* (14), 1297–1304.
- (45) Grycuk, T. *J. Chem. Phys.* **2003**, *119*, 4817–4826.
- (46) Mongan, J.; Svrcek, Seiler, W. A.; Onufriev, A. *J. Chem. Phys.* **2007**, *127*, 185101:1–10.
- (47) Lange, A. W.; Herbert, J. M. *J. Chem. Phys.* **2011**, *134*, 204110:1–15.
- (48) Debye, P.; Hückel, E. *Physik. Z.* **1923**, *24*, 185–206.
- (49) Srinivasan, J.; Trevathan, M. W.; Beroza, P.; Case, D. A. *Theor. Chem. Acc.* **1999**, *101*, 426–434.
- (50) Sigalov, G.; Fenley, A.; Onufriev, A. *J. Chem. Phys.* **2006**, *124*, 124902:1–14.
- (51) For finite ϵ , the corresponding substitutions would be to replace $\int d\vec{s} \sigma_i(\vec{s})$ with $(e^{-1}-1)q_i$. Then, replacing $\vec{r}_j - \vec{s}^{-1}$ with f_{ij} affords the conventional (salt-free) GB model. Although this “derivation” is certainly not rigorous, the equivalence with C-PCM turns out to be exact in the salt-free case. In ref 30, we arrived at this equivalence in a mathematically rigorous way.
- (52) Sigalov, G.; Scheffel, P.; Onufriev, A. *J. Chem. Phys.* **2005**, *122*, 094511:1–15.
- (53) Kirkwood, J. G. *J. Chem. Phys.* **1934**, *2*, 351–361.
- (54) Scopes, R. K. *Protein Purification: Principles and Practice*; Springer-Verlag: New York, 1994.
- (55) Cancès, E.; Mennucci, B.; Tomasi, J. *J. Chem. Phys.* **1997**, *107*, 3032–3041.
- (56) Mennucci, B.; Cancès, E.; Tomasi, J. *J. Phys. Chem. B* **1997**, *101*, 10506–10517.
- (57) Tomasi, J.; Mennucci, B.; Cancès, E. *THEOCHEM* **1999**, *464*, 211–226.
- (58) Cancès, E. In *Continuum Solvation Models in Chemical Physics*; Mennucci, B., Cammi, R., Eds.; Wiley: New York, 2007; pp 29–48.
- (59) For classical point charges contained within a cavity, the IEF-PCM approach is equivalent to the SS(V)PE method introduced by Chipman,^{63,13} although a minor difference exists in the implementation of these two methods for quantum-mechanical solutes.^{13,26}
- (60) Connolly, M. L. *J. Appl. Crystallogr.* **1983**, *16*, 548–558.
- (61) Salsbury, F. R., Jr. *Mol. Phys.* **2006**, *104*, 1299–1309.
- (62) Lotan, I.; Head-Gordon, T. *J. Chem. Theory Comput.* **2006**, *2*, 541–555.
- (63) Chipman, D. M. *J. Chem. Phys.* **2000**, *112*, 5558–5565.